Amino Acids (2011) 40:183–195
DOI 10.1007/s00726-010-0632-1

ORIGINAL ARTICLE

C-terminal amidation of PMAP-23: translocation to the inner membrane of Gram-negative bacteria

Jin-Young Kim · Seong-Cheol Park · Moon-Young Yoon · Kyung-Soo Hahm · Yoonkyung Park

Received: 14 December 2009 / Accepted: 21 April 2010 / Published online: 30 May 2010

Abstract PMAP-23 is a member of the cathelicidin family derived from pig myeloid cells and has potent antimicrobial activity. Amidation of the carboxyl terminus (C-terminus) of an antimicrobial peptide generally enhances its structural stability and antimicrobial activity or decreases its cytotoxicity. The aim of the present study was to investigate the effect of amidation on the mode of action in PMAP-23. Irrespective of amidation, PMAP-23 adopts a helix–hinge–helix structure in a membrane-mimetic environment. The antibacterial activities of PMAP-23C, which had a free C-terminus, and PMAP-23N, which had an amidated C-terminus, were similar against Gram-negative bacteria, reflecting a similar ability to neutralize lipopolysaccharide. However, PMAP-23N assumed a perpendicular orientation across the outer to the inner leaflet of the bacterial inner membrane, while PMAP-23C was orientated parallel to the lipid bilayer, as determined by following the blue shift in tryptophan fluorescence, as well as calcein release from liposomes and SYTOX Green uptake assays. These results suggest that N-terminal amidation of PMAP-23 provides structural stability and increases the peptide's cationic charge, facilitating translocation into the bacterial inner membrane.

Keywords PMAP-23 · Antimicrobial peptide · Lipopolysaccharide · Amidation · Translocation · Membrane bilayer

Abbreviations

LPS	Lipopolysaccharide
PE	L-α-phosphatidylethanolamine
PG	L-α-phosphatidyl-DL-glycerol
CL	Cardiolipin
$DiSC_3$-5	3,3′-Diethylthio-dicarbocyanine iodide
CFU	Colony-forming unit
AMP	Antimicrobial peptide
MTT	3-(4,5-Dimethylthiazol-2-yl)-2,5-diphenyltetrazolium bromide, a tetrazole
TFE	Trifluoroethanol
DMSO	Dimethyl sulfoxide
LB	Luria–Bertani

Introduction

The emergence of microbial pathogens resistant to conventional antibiotics has stimulated a search for new therapeutic drugs (Lehrer and Ganz 1993; Ganz and Lehrer 1999). Antimicrobial peptides (AMPs) are of particular interest because their proposed mode of action does not appear to stimulate rapid development of microbial

J.-Y. Kim and S.-C. Park contributed equally to this work.

J.-Y. Kim · S.-C. Park · K.-S. Hahm (✉) · Y. Park (✉)
Research Center for Proteineous Materials (RCPM), Chosun University, Kwangju, Korea
e-mail: kshahm@chosun.ac.kr

Y. Park
e-mail: y_k_park@chosun.ac.kr

M.-Y. Yoon
Department of Chemistry, Hanyang University, Seoul 133-791, Korea

K.-S. Hahm
Department of Cellular-Molecular Medicine, School of Medicine, Chosun University, Kwangju, Korea

Y. Park
Biotechnology and BK21 Research Team for Protein Activity Control, Chosun University, Kwangju, Korea

resistance (Ganz and Lehrer 1999) and, over the past two decades, numerous AMPs have been identified in both prokaryotes and eukaryotes (for review, see Jenssen et al. 2006; Wong et al. 2007; Bergsson et al. 2005; Park et al. 2008a). AMPs play key roles in the primary host defense against infectious pathogens as a part of the innate immune system widely distributed in nature (Bergsson et al. 2005 and Park et al. 2008a, b). The targets of AMPs are known to be the cytoplasmic membrane and the processes of cell division and macromolecule synthesis, but their precise modes of action are not well understood (Brogden 2005; Zasloff 2002 and Hale and Hancock 2007).

In mammals, neutrophils express, store in cytoplasmic granules and secrete a number of host defense proteins including cathelicidins, which are a family of effectors of innate immunity characterized by a 12-100 residue C-terminal antimicrobial domain linked to an evolutionally conserved N-terminal cathelin-like domain (Zanetti et al. 1995; Shunyi et al. 2008; Borregaard et al. 2007; Lee et al. 2008). Cathelicidin-derived peptides have been further divided into the α-helical [CRAMP (Gallo et al. 1997), SMAP-29 (Bagella et al. 1995), PMAP-37 (Tossi et al. 1995), human CAP18 (Larrick et al. 1995)], Cys-rich protegrins (Zhao et al. 1994), Pro/Arg-rich and Trp-rich subfamilies [Bac5, Bac7 (Gennaro et al. 1989), PR-39 (Storici and Zanetti 1993) and indolicidin (Del Sal et al. 1992)]. All of these peptides show potent antimicrobial activity against bacteria, fungi, parasites and tumor cells and, in most cases, their mechanism of action is membrane disruption (Ramanathan et al. 2002).

Porcine myeloid antibacterial peptide, composed of 23 residues (PMAP-23), was identified from cDNA encoding a putative AMP precursor of porcine myeloid mRNA and belongs to the amphipathic α-helical peptide subgroup of the cathelicidin family (Zanetti et al. 1994). The structure of PMAP-23 is a helix–hinge–helix in membrane-mimetic environments and shows potent killing activity against a broad spectrum of microbial organisms (Park et al. 2002).

Previous studies of amidated peptides have suggested that the net charge, primary sequence and, probably, the secondary structure adopted on contact with biological membranes are important modulators of the peptide's biological activity (Sforça et al. 2004; Apponyi et al. 2004). However, their different modes of action in membrane environments are unclear. C-terminal amidation is one of the post-translational modifications used to enhance the stability and antimicrobial activity of antimicrobial peptides and to bioactivate certain neuropeptides; it is also associated with peptide resistance to enzymatic degradation (Andreu and Rivas 1998; Nguyen et al. 2005).

In the present study, both C-terminal amidated PMAP-23 (PMAP-23N) and non-amidated PMAP-23 (PMAP-23C) were synthesized to investigate the effect of C-terminal amidation on the peptide's mode of action and biological activity against Gram-negative bacterial strains. In addition, we compared the behavior of the two peptides in artificial liposomes and living cells using biological and biophysical assays.

Materials and methods

Materials

LPS (from *Escherichia coli* 0111:B4) was purchased from Sigma Chemical Co. (St. Louis, MO, USA). $DiSC_3$-5 and SYTOX Green were acquired from Molecular Probes (Eugene, OR, USA). PE (L-α-phosphatidylethanolamine), PG (L-α-phosphatidyl-DL-glycerol) and CL (cardiolipin, from *E. coli*) were obtained from Avanti Polar Lipids (Alabaster, AL, USA).

Peptide synthesis and purification

All peptides were synthesized using solid-phase methods with Fmoc (*N*-(9-fluorenyl) methoxycarbonyl)-protected amino acids on a Liberty Microwave Peptide Synthesizer (CEM Co., Matthews, NC, USA). 4-Methyl benzhydrylamine resin and Rink Amide MBHA (Novabiochem) (0.55 mmol/g) were employed to produce the amidated and non-amidated PMAP-23 (RIIDLLWRVRRPQKPKFVTV WVR), respectively. After synthesis of the peptides, the crude peptide was purified on a Waters preparative HPLC system on a Waters 15 μm Deltapak C_{18} column (39 × 300 mm), using an appropriate 0–60% acetonitrile gradient in water with 0.1% trifluoroacetic acid. The purity of the isolated peptide was determined on a Shimadzu analytical HPLC system equipped with a Vydac C_{18} column (4.6 × 250 mm, 300 Å, 5 μm). The molecular masses of the peptides were confirmed using a matrix-assisted laser desorption ionization mass spectrometer (MALDI II, Kratos Analytical Ins.).

Antimicrobial assay

Escherichia coli (ATCC 25922) and *Pseudomonas aeruginosa* (ATCC 15692) were obtained from American Type Culture Collection. *Salmonella typhimurium* (KCTC 1926) and *Proteus vulgaris* (KCTC 2433) were obtained from Korean Collection for Type Cultures. *Escherichia coli* (CCARM 1229 and CCARM 1238) and *Salmonella typhimurium* (CCARM 8009 and CCARM 8013) were obtained from Culture Collection of Antimicrobial Resistance Microbes (Seoul Women's University).

The antibacterial activity of the PMAP-23 peptides was determined using microdilution assays. Briefly, bacteria

were collected in mid-log phase and suspended in PBS (1.5 mM KH_2PO_4, 2.7 mM KCl, 8.1 mM Na_2HPO_4, 135 mM NaCl, pH 7.2) supplemented with 10% appropriate culture media. The peptide with concentrations ranging from 1 to 128 μM, achieved by twofold serial dilution, was added to sterile 96-well plates, after which aliquots of cell suspension (2×10^5 CFU/ml) were added to each well. After incubation for 24 h, the turbidity of the suspensions was measured at a wavelength of 600 nm using a VERSAmax microplate reader (Molecular Devices Co., Sunnyvale, CA, USA) to determine the minimal inhibitory concentration (MIC). The lowest peptide concentration that completely inhibited growth was defined as the MIC. MIC values were calculated as an average of several independent experiments conducted in triplicate (Kim et al. 2007).

Human red blood cell (hRBC) hemolysis

The hemolytic activities of peptides were assessed using hRBCs collected on heparin from healthy donors. The fresh hRBCs were rinsed three times in PBS, collected by centrifugation for 10 min at 800×*g* and resuspended in PBS. The twofold serial peptides diluted with PBS were added to 100 μl of hRBCs suspended in PBS (final RBC concentration, 8% v/v), after which the samples were incubated for 60 min at 37°C with mild agitation and then centrifuged for 10 min at 800×*g*. The absorbance of the supernatants was assessed at 414 nm; the controls for zero (blank) and 100% hemolysis were hRBCs suspended in PBS and 1% Triton X-100, respectively. All measurements were made in triplicate (Park et al. 2008b).

Cytotoxicity

The percentage of growth inhibition was evaluated using MTT (Sigma) assays to measure the numbers of viable HaCaT cells (a spontaneously immortalized human keratinocyte line). A total of 2×10^4 cells/well were seeded into the wells of a 96-well plate and incubated for 24 h. After peptide was added to each well and incubated for 24 h at 37°C, 10 μl of 5 mg/ml MTT were added to the wells and incubated for an additional 4 h. The supernatants were then aspirated, and 50 μl of DMSO were added to dissolve any remaining precipitate. Absorbance was then measured at a wavelength of 570 nm (Park et al. 2008a).

LPS neutralization

Neutralization of the peptides was measured using a chromogenic limulus amebocyte lysate assay (Ried et al. 1996). A constant concentration of LPS (1 ng/ml) was incubated with various concentrations of peptides (0–20 μM) at 37°C in the wells of an apyrogenic sterile microtiter plate. A total of 50 μl of this mixture was then added to equal volumes of limulus amebocyte lysate reagent and this mixture was incubated for 10 min at 37°C. A yellow color developed on addition of 100 μl of chromogenic substrate solution. After stopping that reaction by adding 25% acetic acid, the absorbance was measured at 405 nm.

The effect of LPS on antibacterial activity

Serially diluted peptides (2–64 μM) were incubated with 32 μM LPS (peptide:LPS ratio = 2:1, 1:1 to 1:16) for 1 h at 37°C. The mixtures were then incubated for 2 h under the same conditions after adding suspensions of exponentially growing *E. coli*. Aliquots were then dripped for visualization of bacterial cells (Rosenfeld et al. 2006).

Circular dichroism (CD) analysis

CD spectra were recorded at 25°C on a Jasco 810 spectropolarimeter (Jasco, MD, USA) equipped with a temperature control unit. Aliquots of 50 μM peptide solution were scanned in a 0.1-cm path-length quartz cell. At least five scans were averaged for each sample, and the averaged blank spectra were subtracted. Each spectrum was obtained by averaging five scans in the 250–190 nm wavelength range. All CD spectra are reported in terms of mean residue ellipticity, $[\theta]_{MRW}$, in deg cm^2 $dmol^{-1}$ (Maeng et al. 2001).

Membrane depolarization in *E. coli*

Membrane depolarization was assessed using $DisC_3$-5, a lipophilic potentiometric indicator dye (Papo et al. 2002).

Intact E. coli cells

Escherichia coli were grown to mid-log phase at 37°C with agitation, after which they were washed once in buffer A (20 mM glucose, 5 mM HEPES, pH 7.3) and resuspended to an OD_{600} of 0.05 in buffer A containing 0.1 M KCl. The cells were then incubated with 1 μM $DiSC_3$-5 until stable baseline fluorescence was achieved. PMAP-23 peptides were then added to 480 μl of bacterial suspension, after which changes in fluorescence were continuously recorded (excitation wavelength, 622 nm; emission wavelength, 670 nm) for 30 min.

Spheroplast of E. coli

Spheroplasts of *E. coli* ATCC 25922 bacteria were prepared via an osmotic shock technique (Yanagida et al. 1986). First, cells from cultures grown to an OD_{600} of 0.8 were harvested by centrifugation, washed twice in buffer C

(10 mM Tris/H_2SO_4, 25% sucrose, pH 7.5) and resuspended in buffer C containing 1 mM EDTA. After incubation for 10 min at 20°C with rotary mixing, the cells were harvested by centrifugation, immediately resuspended in ice-cold water and incubated for 10 min at 4°C. The resultant spheroplasts were harvested by centrifugation and resuspended to an OD_{600} of 0.05 in buffer D (20 mM glucose, 5 mM HEPES, 1 M KCl, pH 7.3). Further treatments were conducted as described in the above intact cells except for the concentration of peptide (1–10 μM).

Killing kinetics

Escherichia coli were grown overnight in LB broth and diluted to an OD_{600} of 0.05. PMAP-23 peptides were then added in concentrations corresponding to the membrane depolarization experiment. Bacteria were sampled at defined intervals of 0, 1, 2, 3, 4, 5, 6, 7, 8, 9, 10, 15, 20, 30 or 40 min, after which 20-fold dilutions were plated on LB agar. The plates were then incubated at 37°C, and the colony-forming units (cfu) were counted after 24 h (Pag et al. 2008; Marynka et al. 2007).

SYTOX Green uptake assay

Escherichia coli were grown in LB at 37°C, washed, suspended (2×10^7 cells/ml) in PBS and incubated with 1 μM SYTOX Green for 15 min with agitation in the dark (Mangoni et al. 2004). After the addition of the PMAP-23 peptides, the increase in fluorescence, reflecting the binding of the dye to intracellular DNA, was monitored (excitation wavelength of 485 nm and emission wavelength of 520 nm).

Tryptophan fluorescence blue shift

The fluorescence emission spectrum of Trp residues in the PMAP-23 peptides was monitored in aqueous PBS buffer and in liposomes, composed of PE/PG (7:3, w/w) or PE/PG/CL (7:1.5:1.5, w/w/w). The tryptophan fluorescence measurements were made in a Perkin–Elmer LS55 fluorometer. Each peptide was added to 3 ml of buffer containing from 0 to 0.6 mM liposomes at a molar ratio of 1:300, 1:150, 1:75, 1:37.5 or 1:18.8, and the mixture was allowed to interact for 10 min at 20°C. The fluorescence was excited at 280 nm, and the emission was scanned from 300 to 400 nm. Blue shifts were calculated as the change in the wavelength of the emission maximum in the spectra of the lipid–peptide mixture (Bolen and Holloway 1990).

Quenching of Trp emission by acrylamide

For fluorescence quenching experiments, Trp was excited at 295 nm instead of 280 nm to reduce absorbance by acrylamide (De Kroon et al. 1990). Trp fluorescence was quenched by titration with acrylamide from a 4 M stock solution to a final concentration of 0.2 M in the presence of liposome at a peptide:lipid molar ratio of 1:100 (the concentrations of peptides and phospholipid vesicles were 3 and 300 μM, respectively). Experimental data were plotted according to the Stern–Volmer equation, $F_0/F = 1 + K_{SV} - [Q]$, where F_0 was the fluorescence of the peptide in the absence of acrylamide, F was the fluorescence of the peptide in the presence of acrylamide, K_{SV} was the Stern–Volmer quenching constant, and [Q] was the concentration of acrylamide. Measurements were repeated three times at a given condition to ensure reproducibility.

Calcein release from liposomes

Permeabilization of liposomes by the PMAP-23 peptides was assayed by measuring leakage of entrapped calcein. Liposomes in which calcein was entrapped were prepared for use in dye leakage experiments as follows. Briefly, the dried lipid was pre-hydrated with dye buffer solution (80 mM calcein, 10 mM HEPES, 30 mM NaCl, pH 7.4), vortexed for 1 min and then allowed to stand for 30 min at 50°C. The suspension was then subjected to nine cycles of freeze–thaw to produce large unilamellar vesicles (LUVs) and then extruded 30 times through polycarbonate filters (two stacked 0.2-μm pore-size filters) using an *Avanti* Mini-Extruder (Avanti Polar Lipids inc., Alabaster, AL, USA). Calcein-entrapped vesicles were separated from free calcein by gel filtration chromatography on a Sephadex G-50 column. Calcein-containing LUVs in suspensions containing 60 μM lipids were incubated with various concentrations of the peptide (1–12 μM), after which the fluorescence of the released calcein was assessed at an excitation wavelength of 480 nm and an emission wavelength of 520 nm using a spectrofluorometer (Perkin–Elmer LS55). Complete (100%) release was achieved by the addition of Triton X-100 to a final concentration of 0.1%. Spontaneous leakage was determined to be negligible at this timescale. The experiments were conducted at 25°C. The apparent percentage of calcein release was calculated using the following equation (Ghosh et al. 1998):

$$\text{Release } (\%) = 100 \times (F - F_0)/(F_t - F_0)$$

Calcein release in the presence of LPS

PE/PG (7:3, w/w) and PE/PG/CL (7:1.5:1.5, w/w/w) LUVs containing calcein (80 mM calcein, 10 mM HEPES, 30 mM NaCl, pH 7.4) were prepared using the method described above. In some cases, peptides (0.1 μM) were incubated with LPS (0.1 μM, ratio = 1:1) for 10 min at 37°C prior to adding the mixture to the LUVs (4 μM, peptide:lipid ratio = 1:40). The intensity of the

fluorescence of the released calcein was monitored as a function of time.

Results

Biological activities of PMAP-23 and PMAP-23C

The antibacterial activities of synthetic peptides against susceptible (*E. coli, S. typhimurium, P. aeruginasa* and *P. vulgaris*) and antibiotic-resistant Gram-negative bacteria (*E. coli* CCARM 1229, *E. coli* CCARM 1238, *S. typhimurium* CCARM 8009 and *S. typhimurium* CCARM 8013) were characterized by determining the MICs. As shown in Table 1, both PMAP-23N and PMAP-23C had similar MICs, ranging from 2 to 16 μM and were 10–80 times more potent than ampicillin, a conventional antibiotic, against antibiotic-resistant strains. The peptides were also tested for the extent of their hemolytic activity against hRBCs and their cytotoxic activity against HaCaT cells (a spontaneously immortalized human keratinocyte line). Both PMAP-23N and -23C showed only low levels of hemolytic and cytotoxic activity, even at 100 μM, and no significant difference between the two peptides was detected.

LPS neutralization and the effect of LPS on antibacterial activity

The efficiency of PMAP-23N and -23C in LPS neutralization was assessed using LAL assays, which are generally accepted as representing the ability of molecules to neutralize LPS (Ried et al. 1996). Both PMAP-23N and -23C were found to neutralize LPS in a dose-dependent manner, and no significant difference was seen between them (Fig. 1a). Moreover, their LPS neutralizing activity was related to their antibacterial activity against Gram-negative bacteria. To determine whether the peptides were free or associated with LPS after neutralization, the activity of the peptides against *E. coli* was tested following their preincubation with selected concentrations of LPS. We found that the two peptides exhibited similar antibacterial activity in the presence and absence of LPS (Fig. 1b), suggesting neither PMAP-23N nor -23C associates with LPS, but instead were able to translocate to the inner membrane of Gram-negative bacteria.

Table 1 Biological activities of amidated or non-amidated PMAP-23

Strains	MICs (μM)[a]		Ampicillin
	PMAP-23C[b]	PMAP-23N[c]	
E. coli	4	4	86
S. typhimurium	2	2	22
P. aeruginosa	8	8	–
P. vulgaris	16	16	–
E. coli CCARM 1229	4	4	345
E. coli CCARM 1238	2	2	345
S. typhimurim CCARM 8009	4	4	>345
S. typhimurim CCARM 8013	4	4	>345
Hemolysis (%)[d]	15.4	4.8	–
Cell survival viability (%)[e]	71	75	–

[a] Minimum inhibitory concentration in phosphate buffered saline, pH 7.4

[b] C-terminal, no amidation

[c] C-terminal amidation

[d] Percentage of hemolysis at a concentration of 100 μM

[e] Percentage of HaCaT cell survival at a concentration of 100 μM

Secondary structure of the peptides in membrane environment

Alteration of the secondary structures of PMAP-23N and -23C in buffer (10 mM sodium phosphate, pH 7.2), LPS

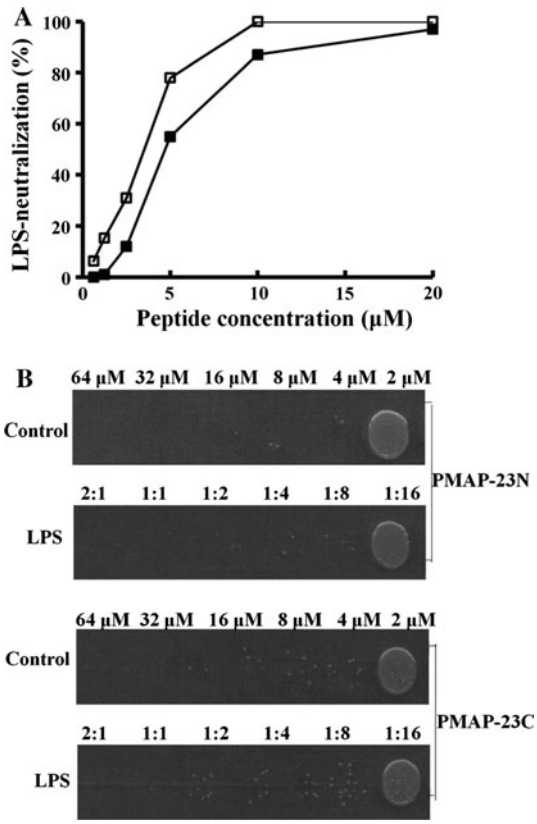

Fig. 1 Dose-dependent neutralization of LPS by PMAP-23N (*open squares*) and PMAP-23C (*filled squares*) as determined by LAL assays (**a**). Effect of LPS on the bactericidal activity of PMAP-23N and PMAP-23C against *E. coli* (**b**) at peptide:LPS ratios from 2:1 to 1:16. Bacterial colony formation was assessed after pre-incubation of LPS with peptides

(outer membrane of Gram-negative bacteria) and 30% TFE (hydrophobic or membrane-mimic environment) was analyzed by CD spectroscopy. As shown in Fig. 2, the two peptides existed as random coils in sodium phosphate buffer and although the helical content differed, they both formed an α-helical structure in LPS and 30% TFE. PMAP-23N had a more stable structure in membrane environments than PMAP-23C.

Depolarization of the bacterial membrane

Peptide-induced membrane permeability leading to dissipation of the transmembrane potential was monitored by measuring increases in fluorescence caused by release of the membrane potential-sensitive fluorescent dye $DiSC_3$-5. In intact *E. coli*, PMAP-23N depolarized the membrane more quickly and to a greater extent than PMAP-23C at the same concentration (Fig. 3A a). In the presence of PMAP-23C, further depolarization was noted on addition of triton X-100 (0.1%), which completely disrupted the membrane, but no further increase in fluorescence was observed on addition of triton X-100 in the presence of PMAP-23N (Fig. 3A b). Interestingly, PMAP-23N and -23C had more dramatically different effects on spheroplast (inner membrane): PMAP-23N induced depolarization of the transmembrane potential at 1 μM, which was a quarter of the MIC, but PMAP-23C did not depolarize the transmembrane potential, even at 8 μM, which was twice the MIC (Fig. 3B).

To investigate the relationship between membrane depolarization and killing rate, we performed bacterial killing assays under the same conditions using the same cell numbers (OD_{600} 0.05) and peptide concentration (8 μM). We found that the kinetics of the bactericidal activity of PMAP-23N was significantly faster than that of PMAP-23C. In fact, at 8 μM concentration, the former peptide led to a decrease of at least 5 log in the CFU after 20 min, while the latter after 40 min (Fig. 3C). We then further analyzed the bactericidal activity based on the interaction between nucleic acids and SYTOX Green, which does not penetrate the inner membrane unless it is disrupted or permeabilized (Roth et al. 1997). Cells treated with 8 μM PMAP-23C did not take up SYTOX Green and only showed a 10% increase in fluorescence at a PMAP-23C concentration of 18 μM. In contrast, a comparable fluorescence increase by PMAP-23N was already present at 1–2 μM peptide (Fig. 3D). These results indicate that PMAP-23N more rapidly interacts with Gram-negative bacteria than PMAP-23C and is more deeply inserted into the inner membrane.

Binding to the membrane

PMAP-23N and PMAP-23C each contain two Trp residues, which we used as intrinsic probes to study the peptide–membrane interactions. In buffer, PMAP-23N and -23C had a fluorescence emission maximum at 352 and 352.5 nm, respectively, which is typical in a polar environment (Zhao and Kinnunen 2002). PE/PG (7:3, w/w) and PE/PG/CL (7:1.5:1.5, w/w/w) (Epand et al. 2008) were used to investigate binding specificity. On addition of PE/PG (7:3, w/w) liposomes, the fluorescence maxima for the two peptides were similarly shifted to shorter wavelengths. In the presence of PE/PG/CL (7:1.5:1.5, w/w/w) liposomes, however, this blue shift was greater for PMAP-23N than for PMAP-23C (Fig. 4a, c). This difference could be

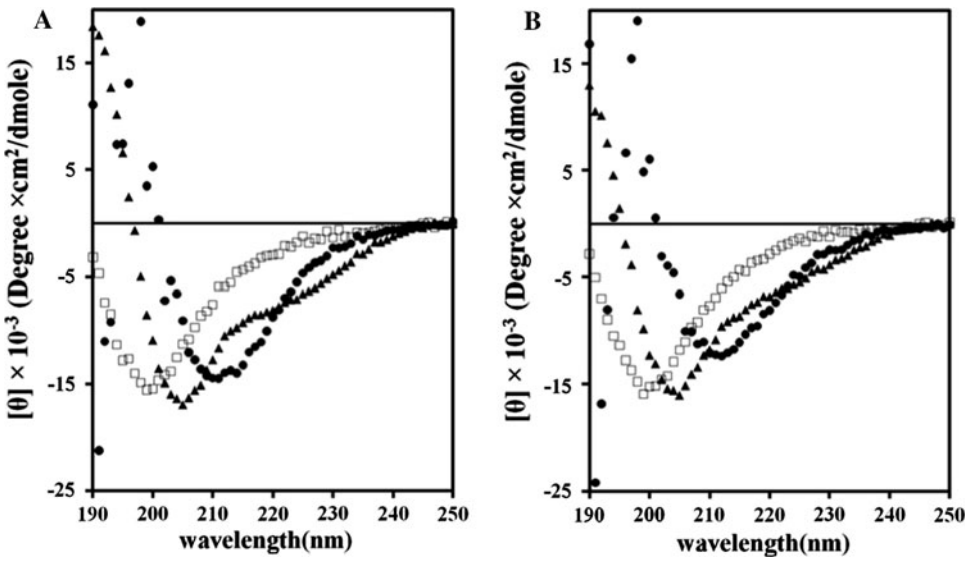

Fig. 2 CD spectra for PMAP-23N (**a**) and PMAP-23C (**b**) recorded in the presence of 10 mM sodium phosphate buffer (*open squares*), 30 μM purified LPS (*filled circles*), or 30% TFE (*filled triangles*)

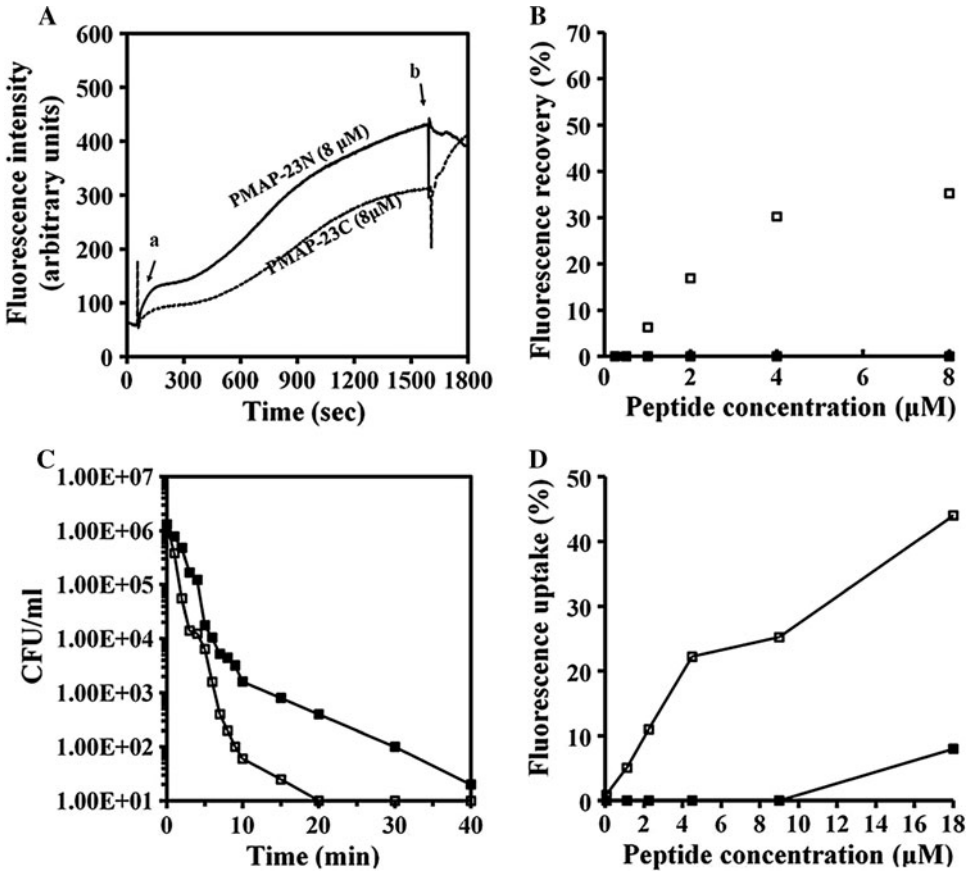

Fig. 3 Peptide-induced permeabilization and killing kinetics in *E. coli*. Depolarization of whole cells in the presence of 8 μM PMAP-23N or PMAP-23C was monitored for 1,800 s at room temperature (**a**). Depolarization of *E. coli* spheroplasts pre-equilibrated for 60 min (**b**). Recovery of $diSC_3$-5 fluorescence was monitored for 120 min (at 5-min intervals) after the peptides were mixed with the bacteria. Killing kinetics of the peptides against *E. coli* (**c**). Bacteria treated with 8 μM PMAP-23N or PMAP-23C were diluted at the indicated times and then plated on LB agar plates. Uptake of SYTOX Green into *E. coli* in the presence of PMAP-23N or PMAP-23C (**d**). The increase in fluorescence was monitored with excitation and emission set at 485 and 520 nm, respectively. The fluorescence obtained in the presence of Triton X-100 was used as 100% uptake. All readings were normalized by subtracting background scattering and the basal fluorescence of the dye. *Open squares* PMAP-23N, *filled squares* PMAP-23C

explained by the fact that the Trp residues of PMAP-23N were located closer to the acyl chains and thus deeper in the membrane.

Translocation into membrane

The observed changes in Trp emission that occurred when the peptides bound to liposomes are indicative of their insertion into the hydrophobic region of the bilayer. To assess the accessibility of liposomes-bound PMAP-23N and -23C, they were treated with acrylamide, a neutral fluorescence quencher that does not interact with the negatively charged head groups of the phospholipids (Epand et al. 2008). Stern–Volmer plots characterizing the quenching of Trp by acrylamide in PE/PG and PE/PG/CL liposomes are depicted in Fig. 4b, d. Although the degree of insertion of both peptides was smaller in PE/PG/CL than in PE/PG, there was a significant gap between the slopes observed with PMAP-23N and -23C.

Release of calcein entrapped within liposomes

The membrane-permeabilizing abilities of PMAP-23N and -23C were investigated by measuring calcein release from anionic PG, PE/PG and PE/PG/CL liposomes. Although the percent leakage increased in a dose-dependent manner after treatment with either PMAP-23N or -23C, the efficiencies of the two peptides differed. PMAP-23N induced greater leakage than PMAP-23C in all liposomes tested: PG (79 vs. 59% leakage), PE/PG (45 vs. 20% leakage) and PE/PG/CL (26 vs. 7.8% leakage) at 4 μM (Fig. 5).

Calcein release by peptides in presence of LPS

To separate the actions of PMAP-23N and -23C at the outer and inner membranes, we tested their ability to release calcien from PE/PG or PE/PG/CL liposomes after pre-incubating the peptides with LPS (Fig. 6). We found that PE/PG liposomes were more susceptible to

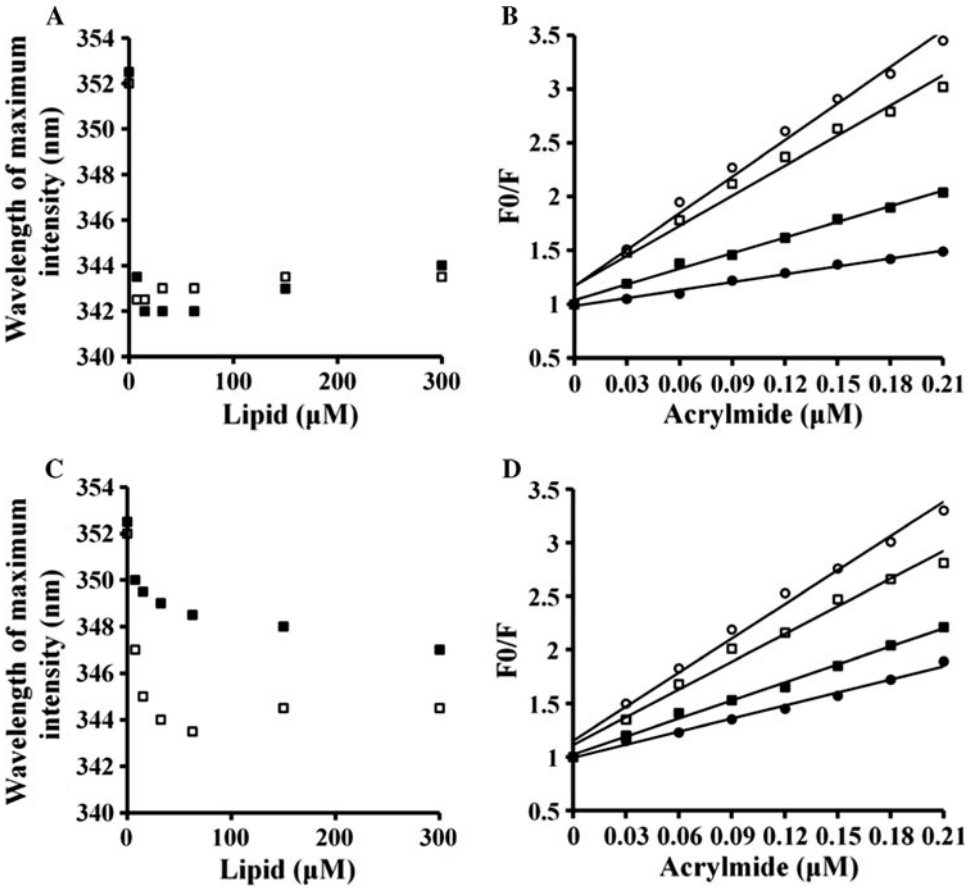

Fig. 4 Wavelengths of maximum PMAP-23N (*open squares*) and PMAP-23C (*filled squares*). Trp fluorescence in the presence of PE/PG (7:3) (**a**) and PE/PG/CL (7:1.5:1.5) (**c**). Quenching of intrinsic PMAP-23N (*circles*) and PMAP-23C (*squares*) Trp fluorescence in buffer and in the presence of PE/PG (7:3) (**b**) and PE/PG/CL (7:1.5:1.5) (**d**) liposomes. The peptide and liposome concentrations were 3 and 300 μM, respectively. *Empty* and *filled symbols* indicate the absence and presence of liposomes, respectively. Each data point is the mean of three independent experiments

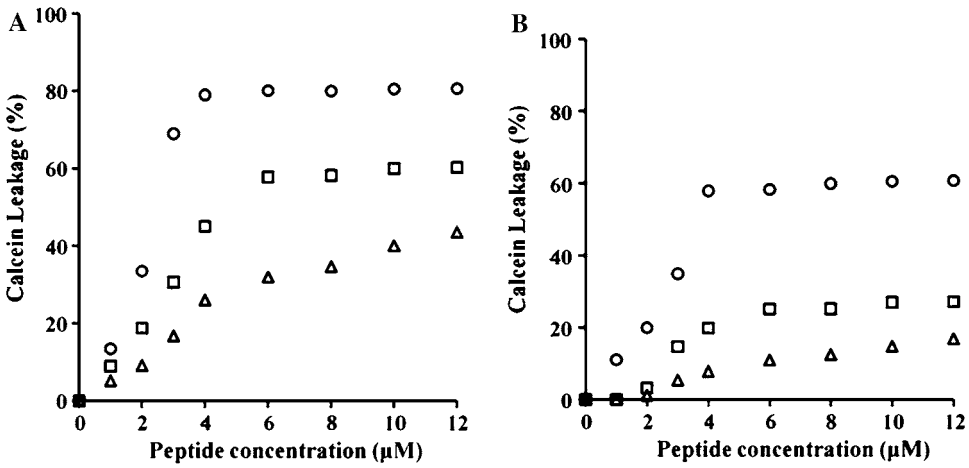

Fig. 5 Dose-dependent leakage of calcein induced by PMAP-23N (**a**) and PMAP-23C (**b**). Calcein release from PG (*open circles*), PE/PG (*open squares*) and PE/PG/CL (*open triangles*) liposomes was defined as the percent release at a lipid concentration of 60 μM. Fluorescence was measured ~30 min after the addition of PMAP-23N or PMAP-23C

permeabilization than PE/PG/CL liposomes and that PMAP-23N permeabilized both liposomes more efficiently than PMAP-23C in the presence of LPS (Fig. 6). Moreover, calcein release from PE/PG/CL liposomes increased exponentially with increasing PMAP-23N concentrations up to a maximum, whereas a slow increase in release was observed with PMAP-23C. This suggests that, in the presence of LPS, PMAP-23N more rapidly interacts with liposomes than PMAP-23C and inserts more deeply than PMAP-23C into the inner membrane, which comprised CL, an anionic phospholipid.

Discussion

AMPs generally have amphipathic and cationic features, which are very important for their interaction with pathogenic bacteria. The amphipathic structure of AMPs

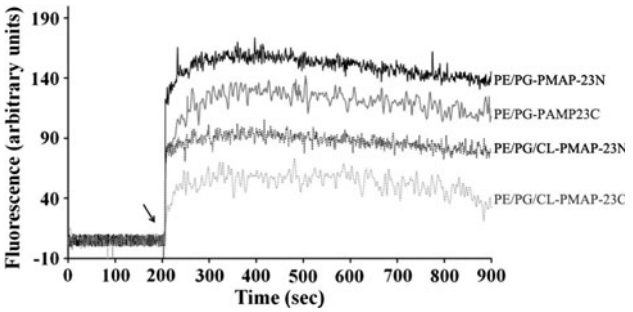

Fig. 6 Time-dependent calcein leakage from 4 μM PE/PG and PE/PG/CL liposomes, induced by 0.1 μM PMAP-23N or -23C pretreated with 0.1 μM LPS. The *arrow* indicates the addition of the peptide-LPS mixture

comprised hydrophilic and hydrophobic amino acids enabling them to match the polar/non-polar interfacial regions of the cell membrane. In addition, the peptide's cationicity promotes interactions with the anionic membrane of bacterial cells. Despite the common features, structures and hydrophobic/hydrophilic balance of AMPs, the variation in their sequences makes it difficult to define their mode of action in detail, i.e., the primary sequences of AMPs contain multiple combinations of hydrophilic and hydrophobic amino acids that have different affinities for the lipid head groups during their initial binding to the membrane and for the fatty acids on insertion/bending. Consequently, a better understanding of the mechanism by which these peptides interact with the membrane is necessary before they can be modified for eventual use as antibiotics.

Natural AMPs from different sources exhibit a variety of posttranslational modifications, including glycosylation (Mackintosh et al. 1998; Bulet et al. 1995; Cociancich et al. 1994), disulfide bonds (Mangoni et al. 1996; Morikawa et al. 1992; Fujii et al. 1993), amidation (Andreu et al. 1983; Mor et al. 1991; Agerberth et al. 1991; Destoumieux et al. 1997), halogenations (Park et al. 1997), addition of D-amino acids (Mignona et al. 1993), methylation (Kokryakov et al. 1993) and phosphorylation (Driscoll et al. 1995; Goumon et al. 1996). Among these, amidation is the most common. Several studies have shown that the activity of AMPs increases following amidation or conversely, decreases following amide removal (Sandvik and Dockray 1999; Katayama et al. 2002; Ali et al. 2001). It has been proposed that the enhanced antibacterial activity exhibited by the amidated forms is associated with a more rigid and extended α-helical structure, as suggested by CD spectra, nuclear magnetic resonance (NMR) spectroscopy and molecular dynamics (MD) simulation (Sforça et al. 2004; Shalev et al. 2002; Dos Santos Cabrera et al. 2008a). Still, the link between amidation and the biological function of AMPs has not been completely defined.

We therefore examined how C-terminal amidation of PMAP-23, which is an amphipathic α-helical peptide in the cathelicidin family, affects its mechanism of action. An earlier report proposed that the N-terminal helix of PMAP-23, which has a helix–hinge–helix structure, first attaches to the hydrophilic head groups of the membrane phospholipid and then the C-terminal helix inserts into hydrophobic region of the membrane (Yang et al. 2006). Moreover, Orioni et al. (2009) recently used a combination of fluorescence spectroscopy and molecular dynamics simulations to determine that PMAP-23C locates below the polar head groups in the membrane and is orientated parallel to the plan of the bilayer. Their findings support the "carpet" model, and they proposed that the mechanism of bilayer destabilization involves the unusual insertion of charged side chains into the hydrophobic core of the membrane. However, because of the composition of the artificial liposomes used by those investigators, their conclusions are only applicable to the inner membrane. Under physiological conditions, AMPs must act on live cells, which have a cell wall, membranes, membrane proteins, cytoplasmic material, etc. Moreover, results from specific bacterial species may not be applicable to all bacteria, as there is considerable variation in the lipid compositions of their membranes, and Gram-negative bacteria are composed of an outer (LPS) and inner (PE/PG or PE/PG/CL) membrane, which have different lipid compositions. In the present study, we investigated the mechanisms of two peptides in living *E. coli* and in artificial liposomes comprising LPS or PE/PG (or PE/PG/CL), the major components of the outer and inner membrane, respectively.

In earlier studies, amidation of dermaseptin S3 was shown to enhance its antimicrobial potency (2- to 10- fold) over a broad array of pathogenic microorganisms and to reduce its hemolytic activity (Mor et al. 1994). In contrast, carboxylation of Eumenitin (Konno et al. 2006) and synthetic EMP-AF1 (Konno et al. 2000) at the C-terminus resulted in a significant reduction in both hemolytic and biological activity. Therefore, we first tested whether C-terminal amidation would influence the lytic activity of synthetic amidated PMAP-23 (PMAP-23N) and non-amidated PMAP-23 (PMAP-23C) against Gram-negative strains. We found no significant difference in their lytic activities, although the activity of PMAP-23N was slightly increased against some bacterial strains, with less hemolytic and cytotoxic activity (Table 1).

We next studied the mechanism of action of PMAP-23 peptides in more detail using *E. coli* to determine the effect of amidation. The mechanism by which AMPs kill or inhibit *E. coli* is known to be initiated by contact with the cell wall or outer membrane. A major component of the outer membrane in Gram-negative bacteria is lipopolysaccharide (LPS), also referred to as endotoxin. LPS is

released from the bacteria during cell division, on cell death and, in particular, when treated with an antibiotic (Hancock and Scott 2000). Macrophages recognize LPS through a LPS-binding protein and then release cytokines into the blood, resulting in septic shock. Notably, several AMPs prevent LPS-induced cytokine induction in macrophages, thereby interrupting the development of septic shock in animal models (Larrick et al. 1995; Gough et al. 1996; Scott et al. 1999; Giacometti et al. 2002). The diphosphoryl head groups of LPS possess a net anionic charge and its acyl chains are hydrophobic. Antimicrobial peptides generally bind to LPS through electrostatic interactions between the cationic amino acids of the peptide and head groups of LPS, which results in the formation of a stable complex through hydrophobic interactions between the hydrophobic amino acids of the peptide and fatty acyl chains of LPS (Li et al. 2004). This interaction ultimately results in the disruption of the LPS layer. In the present study, we found that PMAP-23N and -23C have the same antibacterial activity and similarly neutralized LPS, which indicates that there is a direct correlation between their ability to neutralize LPS and antibacterial activity.

An earlier study suggested that two peptides with the same amino acid composition, but with different structures and hydrophobicities, would exhibit different actions against LPS (Papo and Shai 2005). If the peptides formed oligomers after binding to LPS, they may be unable to insert into the inner membrane. In contrast, preventing the formation of oligomers would allow the peptides to traverse to the inner membrane via the lipid core of LPS (Papo and Shai 2005). To investigate which of these scenarios applies to PMAP-23, we compared the antibacterial potency of PMAP-23N and -23C against *E. coli* after preincubation with LPS. Both peptides displayed similar antibacterial activity in the absence and presence of LPS (Fig. 1b), which suggests that they were able to reach the inner membrane via the LPS lipid core. Thus, LPS apparently does not promote the formation of an oligomeric state. Particularly important is that LPS induces a change in the structure of the peptides from a disordered linear form to an ordered helical form. The helical structure is known to stabilize amphipathic organization, which is critical for the activity of many AMPs (Tossi et al. 2000).

To investigate how PMAP-23N and -23C kill bacteria, we assessed depolarization of the transmembrane potential in intact cells and spheroplasts, the killing kinetics and SYTOX Green uptake by *E. coli*. Although the peptide's antibacterial activities were similar, PMAP-23N displayed more rapid bactericidal kinetics than PMAP-23C, which was consistent with the faster depolarization of intact cells by PMAP-23N. In addition, PMAP-23N induced larger depolarizations than the same concentration of PMAP-23C. These results may have occurred because the increased cationic charge due to amidation increased the attraction of PMAP-23N to the negatively charged cell wall. Interestingly, a difference between the two peptides was observed in the inner membrane of Gram-negative bacteria, as PMAP-23N depolarized the spheroplasts and PMAP-23C did not. As shown in Fig. 3a, b, PMAP-23C perturbed and depolarized the outer membrane, but did not depolarize the inner membrane at the same concentration (8 μM). To confirm this result, bacterial membrane permeabilization in the presence of the peptides was assayed using SYTOX Green, a membrane-impermeant dye that enters bacterial cells and binds to nucleic acids only when both the outer and inner membrane are disrupted or damaged (Mangoni et al. 2004). Although dye uptake after treatment with PMAP-23C increased slightly at four times the MIC, it did not permeabilize the membrane at two times the MIC. By contrast, treatment with PMAP-23N resulted in a dose-dependent increase in dye uptake, which suggests that PMAP-23N can be translocated to the inner membrane of Gram-negative bacteria, but PMAP-23C cannot.

To clearly understand the mechanism of PMAP-23N and -23C, several experiments were performed with artificial liposomes. PE is the major zwitterionic lipid, and CL and PG are major anionic lipids in most bacteria (Epand et al. 2008), although their relative amounts are variable. Generally, vesicle systems composed of PC/PG or PE/PG have been used to mimic the environment of the inner membrane. However, some researchers reported that AMPs display different affinities and modes of action in the two membrane systems (Yang et al. 2008; Som and Tew 2006; Epand et al. 2006). Furthermore, a difference in AMP effects on vesicles was seen in the presence and absence of CL (Epand et al. 2008; Xiong et al. 2005; Epand et al. 2002; Dos Santos Cabrera et al. 2008b). We therefore performed our study using PE, PG and/or CL membrane systems, which were similar in composition to the inner membrane of *E. coli*. Although both peptides showed a similar Trp-blue shift in PE/PG vesicles, PMAP-23N was shifted farther into PE/PG/CL vesicles. In addition, acrylamide quenched PMAP-23N more efficiently than PMAP-23C in both vesicles, indicating that the Trp residues in PMAP-23N inserted more deeply into the hydrophobic region of the inner membrane than did those of PMAP-23C. These differences might be due to the increase of the positive charge by the amidated C-terminus in PMAP-23N (Figs. 3, 4). In addition, our calcein leakage experiment and the observed CD spectra demonstrated that the two peptides acted differently in the inner membrane. If both peptides had a similar affinity and partitioning ability on/in PE/PG/CL liposomes, then the induced calcein leakage should have been similar. However, we observed significantly greater dequenching of calcein fluorescence in the presence of PMAP-23N than in the presence of

PMAP-23C. Moreover, CD spectrometry indicated that although the α-helical structures of PMAP-23N and -23C were similar in the presence of LPS (as mention above), PMAP-23C formed a looser α-helix than PMAP-23N, which adopted a tight α-helical structure in PE/PG/CL liposomes (data not shown). Finally, time-dependent leakage of calcein was measured following pre-incubation of the peptides with LPS to separate the action of the peptide at the outer and inner membranes. Interestingly, addition of PMAP-23C to LPS did not increase the release of entrapped calcein from PE/PG/CL liposomes beyond the basal leak. This could mean that PMAP-23C remained in complex with LPS, or that partitioning activity was not as good as that of PMAP-23N.

The results summarized above may be explained by the difference in the properties of PE and CL. The organization of lipids into a bilayer membrane is controlled by their amphipathic character and intrinsic curvature, and the size ratio of the hydrophilic head groups to hydrophobic acyl tails of the lipids affects membrane curvature (Som and Tew 2006). Lipid composition and lipid ordering are recognized as being highly important to the mechanism of action of AMPs. Although a previous report showed that PMAP-23C-induced calcein release from PC/PG liposomes was dose dependent (Orioni et al. 2009), comparatively less dye was released from the PE/PG liposomes used in our study. This may reflect the fact that PE has a smaller head group than PC and is thus packed more tightly in the membrane bilayer, though both lipids are zwiterionic (Mcintosh 1980). In addition, for some experiments, we added CL to the PE/PG liposomes because CL is the actual lipid composition of the inner membrane of *E. coli* and is the most important factor for distinguishing the amidated from the non-amidated PMAP-23. CL has a stronger anionic charge and forms relatively dense configuration within the liposome organization, while PG is less densely organized (Lewis and McElhaney 2009). Consequently, when the C-terminus of PMAP-23N inserts into the bilayer core, the greater cationic charge due to the presence of CL in the inner leaflet increases the electrostatic attraction of PMAP-23N. As a result, PMAP-23N is oriented anti-parallel to the bilayer plane, while PMAP-23C remains parallel to the bilayer plane.

In summary, Fig. 7 describes the sequential actions of PMAP-23N and -23C from the outer to the inner membrane. During the initial binding to LPS, the peptides neutralized LPS and were altered into a helical structure by interaction with the diphosphoryl head groups (negative charge) and fatty acyl chains (hydrophobic region) of LPS. These helical peptides can transverse the outer leaflet of the outer membrane (LPS), form pore and then move into the periplasm, because they are not aggregated in aqueous solution. Specifically, both peptides displayed different

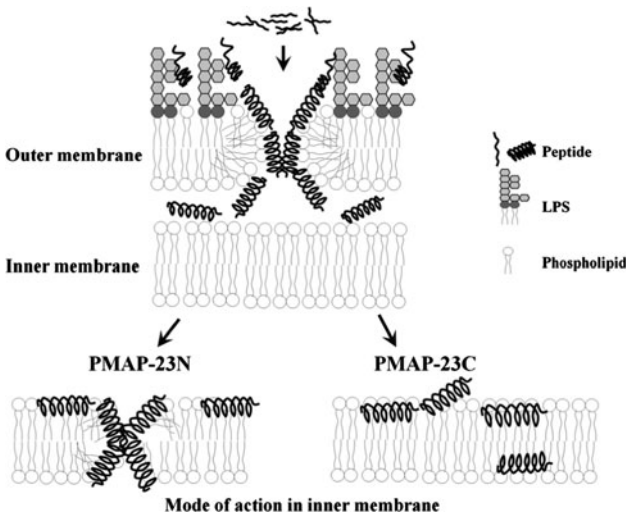

Fig. 7 Schematic model of the action of PMAP-23N and PMAP-23C in Gram-negative bacteria. The two peptides have similar mechanisms of action in/on LPS, but they differ in the inner membrane

action in the inner membrane. PMAP-23N was organized in a perpendicular orientation across the outer to the inner leaflet of the bacterial inner membrane when the C-terminus was inserted into the hydrophobic core of the bilayer. In contrast, PMAP-23C was orientated parallel to the lipid bilayer. The increase of positive charge leads to more helical structure of PMAP-23N in the membrane environment, and it can transverse through the bilayer of the inner membrane because it is composed of a high content of CL. This hypothesis could provide a better understanding of the effects of C-terminal amidation of AMPs on their mechanism of action.

Acknowledgments This work was supported by the Pioneer Research Program for Converging Technology of the Ministry of Education, Science and Technology, Republic of Korea (Grant No. 20100002201) and research funds from Chosun University in 2008.

References

Agerberth B, Lee J-Y, Bergman T, Carlquist M, Boman HG, Mutt V, Jörnvall H (1991) Amino acid sequence of PR-39. Eur J Biochem 202:849–854

Ali MF, Soto AM, Knoop FC, Conlon JM (2001) Antimicrobial peptides isolated from skin secretions of the diploid frog, *Xenopus tropicalis* (Pipidae). Biochim Biophys Acta 1550:81–89

Andreu D, Rivas L (1998) Animal antimicrobial peptides: an overview. Biopolymers 47:415–433

Andreu D, Merrifield RB, Steiner H, Boman HG (1983) Solid-phase synthesis of cecropin A and related peptides. Proc Natl Acad Sci USA 80:6475–6479

Apponyi MA, Pukala TL, Brinkworth CS, Maselli VM, Bowie JH, Tyler MJ, Booker GW, Wallace JC, Carver JA, Separovic F, Doyle J, Llewellyn LE (2004) Host-defence peptides of Australian anurans: structure, mechanism of action and evolutionary significance. Peptides 25:1035–1054

Bagella L, Scocchi M, Zanetti M (1995) cDNA sequences of three sheep myeloid cathelicidins. FEBS Lett 376:225–228

Bergsson G, Agerberth B, Jörnvall H, Gudmundsson GH (2005) Isolation and identification of antimicrobial components from the epidermal mucus of Atlantic cod (*Gadus morhua*). FEBS J 272:4960–4969

Bolen EJ, Holloway PW (1990) Quenching of tryptophan fluorescence by brominated phospholipid. Biochemistry 29:9638–9643

Borregaard N, Sørensen OE, Theilgaard-Mönch K (2007) Neutrophil granules: a library of innate immunity proteins. Trends Immunol 28:340–345

Brogden KA (2005) Antimicrobial peptides: pore formers or metabolic inhibitors in bacteria? Nat Rev Microbiol 3:238–250

Bulet P, Hegy G, Van Dorsselaer A, Hoffmann JA, Hetru C (1995) Insect immunity. The inducible antibacterial peptide diptericin carries two O-glycans necessary for biological activity. Biochemistry 34:7394–7400

Cociancich S, Dupont A, Hegy G, Lanot R, Holder F, Hetru C, Hoffmann JA, Bulet P (1994) Novel inducible antibacterial peptides from a hemipteran insect, the sap-sucking bug *Pyrrhocoris apterus*. Biochem J 300:567–575

De Kroon AI, Soekarjo MW, De Gier J, De Kruijff B (1990) The role of charge and hydrophobicity in peptide–lipid interaction: a comparative study based on tryptophan fluorescence measurements combined with the use of aqueous and hydrophobic quenchers. Biochemistry 29:8229–8240

Del Sal G, Storici P, Schneider C, Romeo D, Zanetti M (1992) cDNA cloning of the neutrophil bactericidal peptide indolicidin. Biochem Biophys Res Commun 187:467–472

Destoumieux D, Bulet P, Loew D, Van Dorsselaer A, Rodrı′guez J, Bachère E (1997) Penaeidins, a new family of antimicrobial peptides isolated from the shrimp *Penaeus vannamei* (Decapoda). J Biol Chem 272:28398–28406

Dos Santos Cabrera MP, Arcisio-Miranda M, Broggio Costa ST, Konno K, Ruggiero JR, Procopio J, Ruggiero Neto J (2008a) Study of the mechanism of action of anoplin, a helical antimicrobial decapeptide with ion channel-like activity, and the role of the amidated C-terminus. J Pept Sci 14:661–669

Dos Santos Cabrera MP, Costa ST, de Souza BM, Palma MS, Ruggiero JR, Ruggiero Neto J (2008b) Selectivity in the mechanism of action of antimicrobial mastoparan peptide Polybia-MP1. Eur Biophys J 37:879–891

Driscoll J, Zuo Y, Xu T, Choi JR, Troxler RF, Oppenheim FG (1995) Functional comparison of native and recombinant human salivary histatin 1. J Dent Res 74:1837–1844

Epand RF, Martinou JC, Fornallaz-Mulhauser M, Hughes DW, Epand RM (2002) The apoptotic protein tBid promotes leakage by altering membrane curvature. J Biol Chem 277:32632–32639

Epand RF, Schmitt MA, Gellman SH, Epand RM (2006) Role of membrane lipids in the mechanism of bacterial species selective toxicity by two alpha/beta-antimicrobial peptides. Biochim Biophys Acta 1758:1343–1350

Epand RM, Rotem S, Mor A, Berno B, Epand RF (2008) Bacterial membranes as predictors of antimicrobial potency. J Am Chem Soc 130:14346–14352

Fujii G, Selsted ME, Eisenberg D (1993) Defensins promote fusion and lysis of negatively charged membranes. Protein Sci 2:1301–1312

Gallo RL, Kim KJ, Bernfield M, Kozak CA, Zanetti M, Merluzzi L, Gennaro R (1997) Identification of CRAMP, a cathelicin-related antimicrobial peptide expressed in the embryonic and adult mouse. J Biol Chem 272:13088–13093

Ganz T, Lehrer RI (1999) Antibiotic peptides from higher eukaryotes: biology and applications. Mol Med Today 5:292–297

Gennaro R, Skerlavaj B, Romeo D (1989) Purification, composition, and activity of two bactenecins, antibacterial peptides of bovine neutrophils. Infect Immun 57:3142–3146

Ghosh JK, Peisajovich SG, Ovadia M, Shai Y (1998) Serum-induced leakage of liposome contents. J Biol Chem 273:27182–27190

Giacometti A, Cirioni O, Ghiselli R, Mocchegiani F, Del Prete MS, Viticchi C, Kamysz W, Lempicka E, Saba V, Scalise G (2002) Potential therapeutic role of cationic peptides in three experimental models of septic shock. Antimicrob Agents Chemother 46:2132–2136

Gough M, Hancock RE, Kelly NM (1996) Antiendotoxin activity of cationic peptide antimicrobial agents. Infec Immu 64:4922–4927

Goumon Y, Strub JM, Moniatte M, Nullans G, Poteur L, Hubert P, Van Dorsselaer A, Aunis D, Metz-Boutigue MH (1996) The C-terminal bisphosphorylated proenkephalin-A-(209–237)-peptide from adrenal medullary chromaffin granules possesses antibacterial activity. Eur J Biochem 235:516–525

Hale JD, Hancock RE (2007) Alternative mechanisms of action of cationic antimicrobial peptides on bacteria. Expert Rev Anti Infect Ther 5:951–959

Hancock RE, Scott MG (2000) The role of antimicrobial peptides in animal defenses. Proc Natl Acad Sci USA 97:8856–8861

Jenssen H, Hamill O, Hancock RE (2006) Peptide antimicrobial agents. Clin Microbiol Rev 19:491–511

Katayama H, Ohira T, Aida K, Nagasawa H (2002) Significance of a carboxyl-terminal amide moiety in the folding and biological activity of crustacean hyperglycemic hormone. Peptides 23:1537–1546

Kim JY, Lee SY, Park SC, Shin SY, Choi SJ, Park Y, Hahm KS (2007) Purification and antimicrobial activity studies of the N-terminal fragment of ubiquitin from human amniotic fluid. Biochim Biophys Acta 1774:1221–1226

Kokryakov VN, Harwig SSL, Panyutich EA, Shevchenko AA, Aleshina GM, Shamova OV, Korneva HA, Lehrer RI (1993) Protegrins: leukocyte antimicrobial peptides that combine features of corticostatin defensins and tachyplesins. FEBS Lett 327:231–236

Konno K, Hisada M, Naoki H, Itagaki Y, Kawai N, Miwa A, Yasuhara T, Morimoto Y, Nakata Y (2000) Structure and biological activities of eumenine mastoparan-AF (EMP-AF), a new mast cell degranulating peptide in the venom of the solitary wasp (*Anterhynchium flavomarginatum micado*). Toxicon 38:1505–1515

Konno K, Hisada M, Naoki H, Itagaki Y, Fontana R, Rangel M, Oliveira JS, Cabrera MP, Neto JR, Hide I, Nakata Y, Yasuhara T, Nakajima T (2006) Eumenitin, a novel antimicrobial peptide from the venom of the solitary eumenine wasp *Eumenes rubronotatus*. Peptides 27:2624–2631

Larrick JW, Hirata M, Balint RF, Lee J, Zhong J, Wright SC (1995) Human CAP 18: a novel antimicrobial lipopolysaccharide-binding protein. Infect Immun 63:1291–1297

Lee JY, Yang ST, Lee SK, Jung HH, Shin SY, Hanm KS, Kim JI (2008) Salt-resistant homodimeric bactenecin, a cathelicidin-derived antimicrobial peptide. FEBS J 275:3911–3920

Lehrer R, Ganz IT (1993) Antimicrobial peptides in mammalian and insect host defense. Curr Opin Immunol 11:23–27

Lewis RN, McElhaney RN (2009) The physicochemical properties of cardiolipin bilayers and cardiolipin-containing lipid membranes. Biochim Biophys Acta 1788:2069–2079

Li P, Wohland T, Ho B, Ding JL (2004) Perturbation of lipopolysaccharide (LPS) micelles by Sushi 3 (S3) antimicrobial peptide. J Biol Chem 279:50150–50156

Mackintosh JA, Veal DA, Beattie AJ, Gooley AA (1998) Isolation from an ant *Myrmecia gulosa* of two inducible *O*-glycosylated proline-rich antibacterial peptides. J Biol Chem 273:6139–6143

Maeng C, Oh MS, Park IH, Hong HJ (2001) Purification and structural analysis of the hepatitis B virus preS1 expressed from *Escherichia coli*. Biochem Biophys Res Commun 282:787–792

Mangoni ME, Aumelas A, Charnet P, Roumestand C, Chiche L, Despaux E, Grassy G, Calas B, Chavanieu A (1996) Change in membrane permeability induced by protegrin 1: implication of disulphide bridges for pore formation. FEBS Lett 383:93–98

Mangoni ML, Papo N, Barra D, Simmaco M, Bozzi A, Di Giulio A, Rinaldi AC (2004) Effects of the antimicrobial peptide temporin L on cell morphology, membrane permeability and viability of *Escherichia coli*. Biochem J 380:859–865

Marynka K, Rotem S, Portnaya I, Cogan U, Mor A (2007) In vitro discriminative antipsedomonal properties resulting from acyl substitution of N-terminal sequence of dermaseptin S4 derivatives. Chem Biol 14:75–85

Mcintosh TJ (1980) Differences in hydrocarbon chain tilt between hydrated phosphatidylethanolamine and phosphatidylcholine bilayers. A molecular packing model. Biophys J 29:237–245

Mignona G, Simmaco M, Kreil G, Barra D (1993) Antibacterial and haemolytic containing D-alloisoleucine from the skin of *Bombina variegata*. EMBO J 12:4829–4832

Mor A, Nguyen VH, Delfour A, Migliore-Samour D, Nicolas P (1991) Isolation, amino acid sequence and synthesis of dermaseptin, a novel antimicrobial peptide of amphibian skin. Biochemistry 30:8824–8830

Mor A, Hani K, Nicolas P (1994) The vertebrate peptide antibiotics dermaseptins have overlapping structural features but target specific microorganisms. J Biol Chem 269:31635–31641

Morikawa N, Hagiwara K, Nakajima T (1992) Brevinin-1 and -2, unique antimicrobial peptides from the skin of the frog, *Ranabrevipoda porsa*. Biochem Biophys Res Commun 189:184–190

Nguyen LT, Schibli DJ, Vogel HJ (2005) Structural studies and model membrane interactions of two peptides derived from bovine lactoferricin. J Pept Sci 11:379–389

Orioni B, Bocchinfuso G, Kim JY, Palleschi A, Grande G, Bobone S, Park Y, Kim JI, Hahm KS, Stella L (2009) Membrane perturbation by the antimicrobial peptide PMAP-23: a fluorescence and molecular dynamics study. Biochim Biophys Acta 1788:1523–1533

Pag U, Oedenkoven M, Sass V, Shai Y, Shamova O, Antcheva N, Tossi A, Sahl HG (2008) Analysis of in vitro activities and modes of action of synthetic antimicrobial peptides derived from an a-helical 'sequence template'. J Antimicrob Chemoth 61:341–352

Papo N, Shai Y (2005) A molecular mechanism for lipospolysaccharide protection of Gram-negative bacteria from antimicrobial peptides. J Biol Chem 280:10378–10387

Papo N, Oren Z, Pag U, Sahi HG, Shai Y (2002) The consequence of sequence alteration of an amphipathic α-helical antimicrobial peptide and its diastereomers. J Biol Chem 37:33913–33921

Park CB, Lee JH, Park IY, Kim MS, Kim SC (1997) A novel antimicrobial peptide from the loach, *Misgurnus anguillicaudatus*. FEBS Lett 411:173–178

Park K, Oh D, Shin SY, Hahm KS, Kim Y (2002) Structural studies of porcine myeloid antibacterial peptide PMAP-23 and its analogues in DPC micelles by NMR spectroscopy. Biochem Biophys Res Commun 290:204–212

Park SC, Kim MH, Hossain MA, Shin SY, Kim Y, Stella L, Wade JD, Park Y, Hahm KS (2008a) Amphipatic α-helical peptide, HP (2–20), and its analogues derived from *Helicobacter pylori*: pore formation mechanism in various lipid compositions. Biochim Biophys Acta 1778:229–241

Park SC, Yoon NC, Kim JY, Park HY, Chae BJ, Shin SY, Cheong H, Park Y, Hahm KS (2008b) Isolation and characterization of an extracellular antimicrobial protein from *Aspergillus oryzae*. J Agric Food Chem 56:9647–9652

Ramanathan B, Davis EG, Ross GR, Blecha F (2002) Cathelicidins: microbicidal activity, mechanisms of action, and roles in innate immunity. Microbes Infect 4:361–372

Ried C, Wahl C, Miethke T, Wellnhofer G, Landgraf C, Schneider-Mergener J, Hoess A (1996) High affinity endotoxin-binding and neutralizing peptides based on the crystal structure of recombinant Limulus antilipopolysaccharide factor. J Biol Chem 271:28120–28127

Rosenfeld Y, Barra D, Simmaco M, Shai Y, Mangoni ML (2006) A synergism between temporins toward Gram-negative bacteria overcomes resistance imposed by the lipopolysaccharide protective layer. J Biol Chem 281:28565–28574

Roth BL, Poot M, Yue ST, Millard PJ (1997) Bacterial viability and antibiotic susceptibility testing with SYTOX Green nucleic acid stain. App Environ Microbiol 63:2421–2431

Sandvik AK, Dockray GJ (1999) Biological activity of carboxy-terminal gastrin analogs. Eur J Pharmacol 364:199–203

Scott MG, Yan H, Hancock RE (1999) Biological properties of structurally related α helical cationic antimicrobial peptides. Infec Immun 67:2005–2009

Sforça ML, SJr Oyama, Canduri F, Lorenzi CCB, Pertinhex TA, Konno K, Souza BM, Palma MS, Ruggiero NJ, Azevedo WF Jr, Spisni A (2004) How C-terminal carboxyamidation alters the biological activity of peptides from the venom of the eumenine solitary wasp. Biochemistry 43:5608–5617

Shalev DE, Mor A, Kustanovich I (2002) Structural consequences of carboxyamidation of dermaseptin S3. Biochemistry 41:7312–7317

Shunyi Z, Liang W, Kenshi Y, Richard LG (2008) Activation of cathepsin L by the cathelin-like domain of protegrin-3. Mol Immunol 45:2531–2536

Som A, Tew GN (2006) Influence of lipid composition on membrane activity of antimicrobial phenylene ethynylene oligomers. J Phys Chem 112:3495–3502

Storici P, Zanetti M (1993) A cDNA derived from pig bone marrow cells contains a sequence identical to the intestinal antimicrobial peptide PR-39. Biochem Biophys Res Commun 196:1058–1065

Tossi A, Scocchi M, Zanetti M, Storici P, Gennaro R (1995) PAMP-37, a novel antibacterial peptide from pig myeloid cells, cDNA cloning, chemical synthesis and activity. Eur J Biochem 228:941–946

Tossi A, Sandri L, Giangaspero A (2000) Amphipathic, α-helical antimicrobial peptides. Biopolymers 55:4–30

Wong JH, Xia L, Ng TB (2007) A review of defensins of diverse origins. Curr Protein Pept Sci 8:446–459

Xiong YQ, Mukhopadhyay K, Yeaman MR, Adler-Moore J, Bayer AS (2005) Functional interrelationships between cell membrane and cell wall in antimicrobial peptide-mediated killing of *Staphylococcus aureus*. Antimicrob Agents Chemother 49:3114–3121

Yanagida N, Uozumi T, Beppu T (1986) Specific excretion of *Serratia marcescens* protease through the outer membrane of *Escherichia coli*. J Bacteriol 166:937–994

Yang ST, Jeon JH, Kim Y, Shin SY, Hahm KS, Kim JI (2006) Possible role of a PXXP central hinge in the antibacterial activity and membrane interaction of PMAP-23, a member of cathelicidin family. Biochemistry 25:1775–1784

Yang L, Gordon VD, Trinkle DR, Schmidt NW, Davis MA, DeVries C, Som A, Cronan JE Jr, Tew GN, Wong GC (2008) Mechanism of a prototypical synthetic membrane-active antimicrobial: efficient hole-punching via interaction with negative intrinsic curvature lipids. Proc Natl Acad Sci USA 105:20595–20600

Zanetti M, Storici P, Tossi A, Scocchi M, Gennaro R (1994) Molecular cloning and chemical synthesis of a novel antimicrobial peptide derived from pig myeloid cells. J Biol Chem 269:7855–7858

Zanetti M, Gennaro R, Romeo D (1995) Cathelicidins: a novel family with a common proregion and a variable C-terminal antimicrobial domain. FEBS Lett 374:1–5

Zasloff M (2002) Antimicrobial peptides of multicelluar organisms. Nature 415:389–395

Zhao H, Kinnunen PKJ (2002) Binding of the antimicrobial peptide temporin L to liposomes assessed by Trp fluorescence. J Biol Chem 277:25170–25177

Zhao C, Liu L, Lehrer RI (1994) Identification of a new member of the protegrin family by cDNA cloning. FEBS Lett 346:285–288